

PUBLICATION II

**Explicit temperature treatment in  
Monte Carlo neutron tracking routines –  
first results**

In proc. PHYSOR-2012, Knoxville, TN, Apr. 15–20 2012.  
Copyright 2012 by the American Nuclear Society.  
Reprinted with permission from the publisher.

## EXPLICIT TEMPERATURE TREATMENT IN MONTE CARLO NEUTRON TRACKING ROUTINES — FIRST RESULTS

**Viitanen Tuomas and Leppänen Jaakko**  
VTT Technical Research Centre of Finland  
P.O. Box 1000, FI-02044 VTT, Finland  
tuomas.viitanen@vtt.fi; jaakko.leppanen@vtt.fi

### ABSTRACT

This article discusses the preliminary implementation of the new explicit temperature treatment method to the development version Monte Carlo reactor physics code Serpent 2 and presents the first practical results calculated using the method. The explicit temperature treatment method, as introduced in [1], is a stochastic method for taking the effect of thermal motion into account on-the-fly in a Monte Carlo neutron transport calculation. The method is based on explicit treatment of the motion of target nuclei at collision sites and requires cross sections at 0 K temperature only, regardless of the number of temperatures in the problem geometry. The method includes a novel capability of modelling continuous temperature distributions.

Test calculations are performed for two test cases, a PWR pin-cell and a HTGR system. The resulting  $k_{\text{eff}}$  and flux spectra are compared to a reference solution calculated using Serpent 1.1.16 with Doppler-broadening rejection correction [2]. The results are in very good agreement with the reference and also the increase in calculation time due to the new method is on acceptable level although not fully insignificant. On the basis of the current study, the explicit treatment method can be considered feasible for practical calculations.

*Key Words:* Monte Carlo, tracking routine, rejection, on-the-fly, Doppler-broadening

### 1. INTRODUCTION

The traditional approach to temperature modelling in Monte Carlo neutron tracking routines is based on pre-generated, Doppler-broadened cross sections. Each material zone is associated with a temperature to which the cross section libraries are prepared beforehand using cross section processing codes such as NJOY [3] or pre-processing techniques [4,5]. In case the user of a reactor physics code wants to increase the amount of detail in the temperature modelling, the geometry has to be split into smaller homogeneous zones, each assigned with a different set of cross sections that need to be stored in the computer memory. If the number of different temperatures or the number of nuclei appearing in the problem is large, the memory usage may become a practical limitation. The importance of detailed temperature modelling is emphasized in multiphysics calculations.

Different means of avoiding this memory limitation have been studied recently. Trumbull et al. studied a method in which cross sections at arbitrary temperatures are obtained by interpolating between tabulated values [6]. However, to reach high accuracy, this method requires a narrow spacing between the different temperatures. Yesilyurt et al. have developed an efficient on-the-fly Doppler-broadening method that is based on the multi-level Adler-Adler resonance representation [7]. This method is able to reach high accuracy in practically no extra calculation time, but requires the resonances to be presented using the Adler-Adler formalism.

This study deals with a new approach to the problem, introduced in [1]. This temperature treatment method is an on-the-fly tracking technique, which takes the thermal motion of target nuclei into account explicitly by making a coordinate transform to target-at-rest frame at each collision site. The fact that the total cross section becomes a distributed quantity is handled using rejection sampling techniques.

The new method is able to model arbitrary temperatures with only 0 K continuous-energy cross sections available. As a novel feature, the explicit treatment method removes the homogeneity requirement for cross section temperatures, consequently providing for rigorous modelling of continuous temperature distributions. Because of the way the target velocities are sampled and collision point candidates accepted, the target velocities at accepted collision sites can be re-utilized as such in the free gas thermal treatment for thermal scattering. The secondary particle distributions become automatically the same as if calculated using the free gas treatment with Doppler-broadening rejection correction (DBRC) [2].

Currently, the method is not compatible with the thermal scattering laws, which significantly limits its applicability to realistic reactor calculations. Also the usage of the method with the unresolved region probability table treatment is not yet discussed. In addition, the method is only applied in homogeneous temperature zones despite the capability to model continuous temperature distributions.

The current study discusses the preliminary implementation of the method to the development version of the Monte Carlo reactor physics code Serpent 2 [8] and presents the very first results calculated using the method. The explicit treatment method is shortly introduced in Section 2 and details of the first implementation are discussed in Section 3. The pin-cell and HTGR test cases together with simulation results are presented in Section 4 and the last Section 5 is left for conclusions.

## 2. EXPLICIT TREATMENT METHOD

In a nutshell, the explicit treatment method is based on sampling the neutron path lengths from a majorant cross section in which the effect of thermal motion on the variation of total cross section is taken into account (i.e. majorant at  $E$  equals the largest possible value assigned for the total cross section within the range of thermal motion around  $E$ ). At each collision site the target nuclide is first sampled according to the nuclide-wise majorants. After this, the velocity of the target nuclide is sampled and the relative velocity of the incident neutron to the target nuclide is calculated. Finally, the collision point is rejected or accepted according to the nuclide-wise 0 K total cross section corresponding to the relative velocity. In the case of an accepted collision the procedure continues by reaction sampling using 0 K cross sections of the partial reactions.

This section introduces the methodology of the explicit treatment method as-is. A more detailed description with more thorough discussion can be found in Reference [1].

## 2.1. Calculating the majorant

The majorant used in the sampling of the path lengths must satisfy

$$\Sigma_{\text{maj}}(E) > \sum_n g_n(E) \Sigma_{\text{tot},n}^0(E', x) \quad \forall E', \quad (1)$$

where  $E$  is the energy of the incident neutron,  $\Sigma_{\text{maj}}$  is the majorant cross section of a material zone,  $\Sigma_{\text{tot},n}^0$  is the 0 K total cross section of nuclide  $n$  and  $E'$  is the energy corresponding to the relative velocity of the incident neutron to the target. The temperature-initiated increase in potential scattering cross section is taken into account using the correction factor

$$g_n(E, T) = \left( 1 + \frac{1}{2\lambda_n(T)^2 E} \right) \operatorname{erf} \left( \lambda_n(T) \sqrt{E} \right) - \frac{e^{-\lambda_n(T)^2 E}}{\sqrt{\pi} \lambda_n(T) \sqrt{E}} \quad (2)$$

$$\lambda_n(T) = \sqrt{\frac{A_n}{kT}}, \quad (3)$$

where  $A_n$  is the weight ratio of nuclide  $n$  to the neutron mass  $M$ ,  $k$  is the Boltzmann constant and  $T$  is the temperature of the material [9]. Since  $E'$  is a variable depending on the velocities of the neutron and target, its range of variation must be taken into account when calculating the majorant cross section.

The variation of  $E'$  depends strongly on the mass of the nuclide and, therefore, it is necessary to calculate the majorants for each nuclide separately. The nuclide-wise majorants  $\Sigma_{\text{tot},n}^0$  are formed in a similar manner as  $\sigma_s^{\text{max}}(v_\xi, 0)$  in Reference [2]. Basically, the majorant for nuclide  $n$  satisfies

$$\Sigma_{\text{maj},n}(E) = g_n(E) \max_{E_\xi \in [(\sqrt{E}-4/\lambda_n(T))^2, (\sqrt{E}+4/\lambda_n(T))^2]} \Sigma_{\text{tot},n}^0(E_\xi) \quad (4)$$

for each incident neutron energy  $E$ . In case the temperature inside material zone is non-uniform,  $T$  in (4) must be chosen as the maximum temperature  $T_{\text{max}}$  within the material region.

The procedure in (4) involves an assumption that the kinetic energies of target nuclei remain smaller than  $16/\lambda_i(T)^2$ . If nuclide velocities are assumed to obey the Maxwell-Boltzmann (MB) distribution, this assumption omits about a proportion of  $5 \cdot 10^{-7}$  of the most energetic nuclei. Consequently, the inequality in (1) does not necessarily apply for all  $E'$ . This cut-off condition was first introduced in the NJOY SIGMA1 module [10].

After the nuclide-wise majorants have been calculated using (4), the material majorant is obtained simply as the sum of the nuclide-wise majorants

$$\Sigma_{\text{maj}}(E) = \sum_n \Sigma_{\text{maj},n}(E). \quad (5)$$

## 2.2. Sampling the target nuclide and velocity

Since the velocity of the target nuclide depends on its mass, the target nuclide has to be sampled at each collision site before the velocity sampling is possible. Target nuclide  $n$  is sampled with

probability

$$P_n = \frac{\Sigma_{\text{maj},n}(E)}{\Sigma_{\text{maj}}(E)}. \quad (6)$$

After this the target velocity  $V_t$  and cosine between the directions of the incident neutron and target  $\mu$  are sampled from distribution

$$f(V_t, \mu) = \frac{v'}{2v} f_{\text{MB}}(V_t), \quad (7)$$

where  $v$  is the velocity of the neutron,

$$v' = \sqrt{v^2 + V_t^2 - 2vV_t\mu} \quad (8)$$

is the relative velocity of the neutron to the target nuclide and  $f_{\text{MB}}$  is the Maxwell-Boltzmann distribution

$$f_{\text{MB}}(V_t) = \frac{4}{\sqrt{\pi}} \gamma^3 V_t^2 e^{-\gamma^2 V_t^2} \quad (9)$$

$$\gamma(T, A_n) = \sqrt{\frac{A_n M}{2kT}}. \quad (10)$$

Distribution 7 is the same as that used in the free gas thermal treatment of MCNP and consequently also the sampling procedure is the same as described in [9].

It should be noted that here temperature  $T$  is the local temperature at the collision site  $x$ , i.e.  $T(x)$ .

### 2.3. Rejection and reaction sampling

The procedure continues with rejection sampling in which the 0 K total cross section corresponding to the sampled relative energy  $E' \sim v'$  is compared to the nuclide-wise majorant. Again, the low-energy effects must be taken into account with the  $g_n(E)$ -factor for the 0 K cross section. The collision point is accepted with probability

$$P_{\text{acc}} = \frac{g_n(E, T(x), A_n) \Sigma_{\text{tot},n}^0(E', x)}{\Sigma_{\text{maj},n}(E)}. \quad (11)$$

In the case of a rejection the procedure restarts from beginning by sampling of a new path length starting from the previous collision point candidate  $x$ .

If the collision point is accepted, the rejection sampling is followed by reaction sampling that is done in the target-at-rest frame using only the 0 K cross sections. Hence, the probability for reaction  $i$  is simply

$$P_i = \frac{g_n(E, T(x)) \Sigma_{i,n}^0(E', x)}{g_n(E, T(x)) \Sigma_{\text{tot},n}^0(E', x)} = \frac{\Sigma_{i,n}^0(E', x)}{\Sigma_{\text{tot},n}^0(E', x)}. \quad (12)$$

### 3. PRELIMINARY IMPLEMENTATION IN SERPENT

There are several ways in which the new method can be implemented in the Monte Carlo tracking routine, but the main requirements are that each nuclide is assigned with a majorant cross section (4), that accounts for the variation in the interaction probability due to thermal motion, and that the sampling of neutron path lengths is based on macroscopic cross sections (5), calculated by summing over these majorants for each material. The rejection sampling additionally requires microscopic 0 K cross sections, adjusted by the correction factor (2) at low energies.

While still studying the feasibility and the best practices for implementing the methodology in the Serpent code, it was decided to take a somewhat simplistic multi-group approach to the problem. The energy spectrum is divided into a number of discrete groups with equal lethargy width. Each nuclide total cross section is assigned with a multi-group majorant, defined by taking the maximum point-wise value within the group boundaries that are extended with the effect of thermal motion as in (4) (see Figure 3 below). Macroscopic material-wise totals are pre-calculated using the same multi-group structure, by summing over the constituent nuclei.

The tracking routine proceeds in the usual way, using the multi-group material totals for sampling path lengths, with additional rejection sampling performed with the probability given by the ratio of point-wise and multi-group total cross sections of the collided nuclide. The method works with and without the explicit temperature treatment. The only difference is that when the method is used, the thermal motion is taken into account in the calculation of the multi-group majorants and in the rejection sampling once the target nuclide is selected. The multi-group approach simplifies and speeds up the calculation of the majorant cross sections. It also enables the use of pre-calculated majorant data without significantly increasing the memory demand. \* The majorant data is generated for each problem separately at runtime. In the present implementation a high number of 40000 energy groups was used for fast calculation. The number can be easily reduced in case memory consumption becomes a problem. The routine can also be implemented without any pre-calculated cross sections, but performing the same calculations during the tracking routine considerably increases the overall running time, especially if the number of nuclei is large.

The following step-by-step example illustrates the rejection sampling procedure when conventional surface-tracking is used for transporting the neutron to the next collision point. Assume that the neutron crosses the boundary surface of a  $\text{UO}_2$  fuel pin in 900 K temperature and enters the material with 1 eV energy. The cross sections in the thermal energy range are plotted in Figure 3. The algorithm proceeds as follows:

1. The distance to the next collision site inside the material is sampled using the macroscopic total cross section of the medium. In this case, the value used is the multi-group total, at about 0.54 1/cm (black curve in Figure 3a).
2. Assuming that the sampled path length is shorter than the distance to the material boundary, the neutron is moved to the collision site. The target nuclide is selected, with probabilities given by the ratios of the corresponding multi-group totals. In this case, the probabilities of colliding with U-235, U-238 and O-16 are 27%, 40% and 33%, respectively.

---

\*Memory usage per material region becomes important in large burnup calculation problems, involving thousands of depletion zones. Minimizing the memory demand is essential for extending the burnup calculation capabilities of the Serpent code from 2D lattice physics to 3D core-level calculations, which is one of the goals set for the development of Serpent 2.

3. Assume that the sample results in a collision with U-235. The relative velocity between the neutron and the target nuclide is sampled from distribution (7) with  $T = 900$  K and  $A_n = 235.04$ . Coordinate transformation to target-at-rest frame essentially results in a new energy, at which the cross sections are evaluated from here on.
4. Rejection sampling is performed by correcting the zero-kelvin total cross section with the factor  $g(1.0 \text{ eV}, 900 \text{ K}) = 1.0002$  (2) and comparing the result with the nuclide-wise multi-group majorant (black solid and dashed curves in Figure 3b). Assuming that the coordinate transformation results in a temperature-corrected energy of 1.1 eV, the probability of accepting the collision point is about 88%.
5. If the collision is rejected, the procedure restarts from step 1. If the collision is accepted, the reaction mode is sampled, with probabilities given by the ratios of the zero-kelvin microscopic cross sections. In this case the probabilities of fission, capture and elastic scattering are 17%, 74% and 9%, respectively.

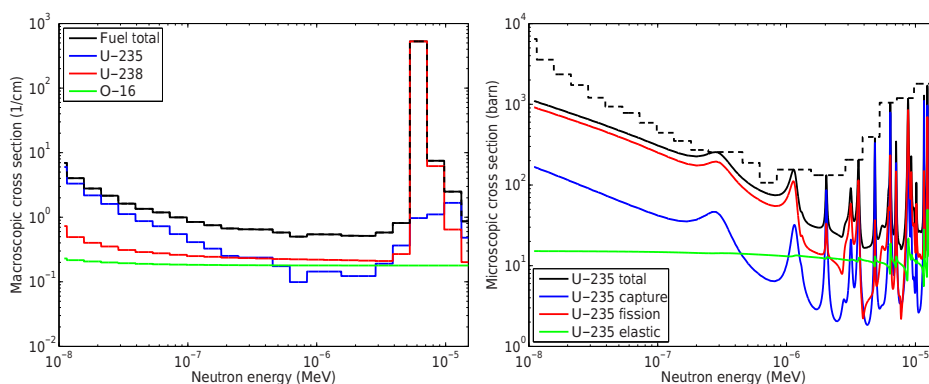


**Figure 1. Left(a): Macroscopic multi-group cross sections used for sampling the target nuclide after collision in fuel. Right(b): Microscopic cross sections used for rejection sampling and selecting the reaction mode. The number of energy groups has been significantly reduced in this example for the sake of clarity.**

As it was previously mentioned, the sampled target velocities can be used also in the calculation of the collision kinetics in case an elastic scattering occurs. It is, therefore, reasonable to take the target motion into account in elastic scatterings throughout the whole energy spectrum even though the free gas treatment is usually limited to energies lower than a cut-off value [8,9].

To get results consistent with NJOY-broadened effective cross sections and to save some calculation time, the velocity of the target nuclide is set to zero for threshold reactions, above the boundary of unresolved resonance region and at energies  $> 1$  MeV [3]. The calculation of the low energy correction factor (2) was also slightly optimized in the implementation. Its value is approximated with 1 if  $\lambda\sqrt{E} > 22$  and with

$$g_n(E) = 1 + \frac{1}{2\lambda_n^2 E} \quad (13)$$

if  $\lambda\sqrt{E} > 2.57$ . Otherwise, the factor is calculated the hard way, i.e. using Equation (2). The relative errors of these approximations remain smaller than 0.001. Quite similar approximations have been used also in MCNP5-1.40 [9].

Although the explicit temperature treatment offers a rigorous approach to the neutron transport problem using only zero-kelvin cross sections, it results in certain limitations regarding the Monte Carlo method and the procedures used in the Serpent code. The most significant methodological limitation is related to the use of the track-length estimate of neutron flux in the calculation of reaction rates, which is based on the assumption that cross sections remain constant over the sampled path length. This is not the case when the relative neutron energy becomes a statistically distributed quantity. To overcome the problem, flux integrals must be calculated using the collision estimator, which uses cross sections only at discrete collision points. Other limitations, related to Serpent-specific methods, are discussed with the example cases in Section 4.

#### 4. TEST CASES AND RESULTS

The Serpent code is optimized for performance in lattice physics applications, and one of the methods used for speeding up the tracking routine and the calculation of macroscopic reaction rates for homogenization is the use of pre-calculated material-wise total cross sections (total, total absorption, total fission, etc.). These cross sections cannot be used with the explicit temperature treatment routine, which immediately reduces the performance when the code is used for group constant generation. In order to present a fair estimate for the overhead caused by the new routine, the performance comparisons should be carried out to calculations without similar optimization. The methodology is validated by comparing analog  $k_{\text{eff}}$  estimators and flux integrals, which doesn't require additional access to cross sections.

The validity of the method was tested by examining two thermal systems: a PWR pin-cell and a HTGR system consisting of 6 compacts around a coolant channel. The systems are modelled using Serpent 2 with the explicit temperature treatment method and the results are compared to a reference calculated with Serpent 1.1.16 [8]. Both of the cases were modelled without the probability table treatment for unresolved resonances and without thermal scattering libraries. Additionally, the Doppler-Broadening Rejection Correction method was used for  $^{238}\text{U}$  while generating the reference results.

The test calculations with the explicit treatment method were performed using a high-resolution JEFF-3.1.1 -based cross section data at 0 K, reconstructed using 0.001 tolerance for nuclei other than  $^{238}\text{U}$  for which a tolerance of 0.003 was used<sup>†</sup>. The reference results were calculated with JEFF-3.1.1 -based libraries with 0.001 reconstruction tolerance used for all nuclei. The same 0 K library with 0.001 / 0.003 reconstruction tolerances was also used together with DBRC in the reference calculations.

Performance measures for the test calculations are performed separately in subsection 4.3.

---

<sup>†</sup>For an unknown reason, NJOY 99.336 was not able to process  $^{238}\text{U}$  in 0 K temperature to reconstruction tolerances smaller than 0.003.

#### 4.1. PWR pin-cell

The first of the test cases involves an ordinary PWR pin-cell in a square lattice. The linear power of the rod was assumed to be 254 W/cm and the corresponding temperature distribution was calculated with the VTT-modified version of the fuel performance code ENIGMA [11,12]. The fuel temperature is modelled by approximating the realistic continuous temperature profile with a 5-step profile.

Temperatures of the fuel zones were adjusted to the exact values using the Doppler-preprocessor of Serpent [5]. The fuel rod properties are listed in Table I and the step function for fuel temperature is defined in Table II. Altogether 250 million active neutron histories were calculated in 5000+20 cycles.

**Table I. Properties for the PWR pin-cell test case.**

Fuel radius	0.41443 cm	Cladding thickness	0.06365 cm
Fuel enrichment	3.48 w-% $^{235}\text{U}$	Cladding material	Zr with 1 w-% Nb
Fuel centerline T	1329 K	Cladding T	579 K
Fuel surface T	738 K	Water density	0.7207 g/cm <sup>3</sup>
Gas gap	0.00727 cm	Water temperature	579 K
Lattice pitch	1.295 cm		

**Table II. Temperature distribution used in the modelling of the fuel in the pin-cell.**

Zone	Outer radius	Temperature
1	0.16586 cm	1275 K
2	0.27638 cm	1129 K
3	0.33162 cm	983 K
4	0.38684 cm	865 K
5	0.41443 cm	772 K

The calculated flux spectrum of the pin-cell case is plotted and compared to reference in Figure 2. To put the accuracy of the method into perspective, the same comparison was performed against a Serpent 1.1.16 spectrum calculated without the DBRC. The analog estimate for  $k_{\text{eff}}$  was  $1.34669 \pm 0.00008$  when calculated with the explicit treatment method and  $1.34644 \pm 0.00008$  in the reference case. This corresponds to a reactivity difference of about  $13 \pm 9$  pcm, which is of the same magnitude as the statistical deviation.

#### 4.2. HTGR

The second test case is based on a High Temperature Gas Cooled Reactor (HTGR) benchmark [13]. The calculations were performed for fresh prismatic fuel for which the input file

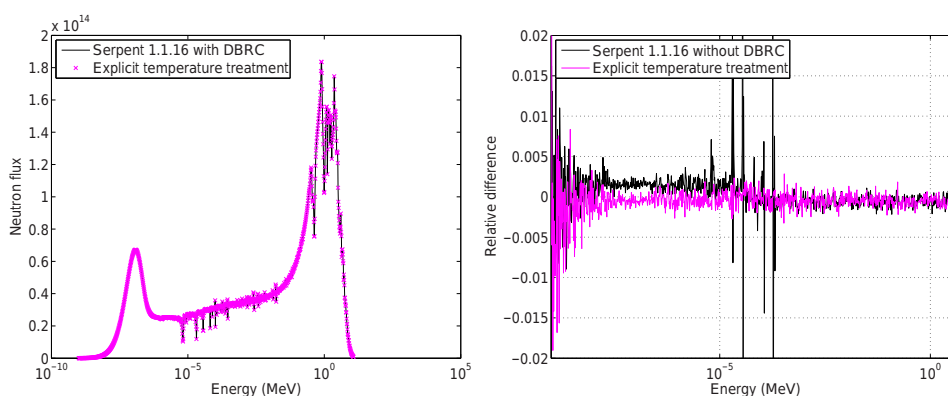


**Figure 2. Left: Flux spectrum of the pin-cell case. Right: Differences in the flux spectra compared to Serpent 1.1.16 with DBRC.**

is available at the Serpent website [8]. In this example case the lattice is modelled with 6 compacts in a graphite matrix surrounding a coolant channel full of helium. The lattice is extended to infinity using periodic boundary conditions. The material temperatures in the input were modified such that fuel in the fuel particles is in 1800 K temperature, all other solid materials are in 1200 K temperature and helium is in 900 K temperature.

While calculating the reference results, it was noticed that the 400 kT free gas treatment (FGT) threshold of Serpent, as adopted from MCNP [9], is too low for this test case and consequently causes significant bias in the results compared to the explicit treatment method in which the target motion is taken into account throughout the whole energy spectrum. Consequently, Serpent 1.1.16 was modified such that FGT was extended to all energies and this modified version was used to calculate the reference results. The HTGR simulations were carried out using 100 million active neutron histories in 5000+10 cycles.

The flux spectrum and differences in the spectra are plotted in Figure 3. Analog  $k_{\text{eff}}$  estimate for the HTGR case was  $1.28296 \pm 0.00010$  in the reference calculation and  $1.28266 \pm 0.00010$  when calculated with the explicit treatment method. The reactivity difference is, thus, about  $18 \pm 15$  pcm which cannot be distinguished from the statistical deviation in practice.

### 4.3. Performance

To evaluate the feasibility of the method in practical calculations, it is worthwhile to compare the calculation times of the reference cases to those of the explicit treatment method. As it was mentioned earlier, the comparison between the explicit method and reference is fair when the optimization in Serpent is somewhat reduced. The righteous level of optimization is obtained when utilizing the optimization mode 2 in Serpent 2 [14]. However, to put the results into perspective, the running times are provided also for the reference cases calculated in Sections 4.1 and 4.2.

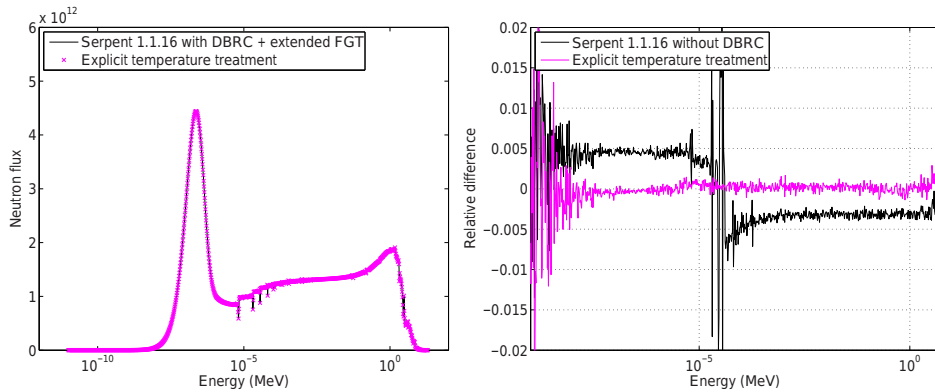


**Figure 3. Left: Flux spectrum of the pin-cell HTGR case. Right: Differences in the flux spectra compared to Serpent 1.1.16 with DBRC and extended Free Gas Treatment.**

The pin-cell cases were calculated using 250 million neutrons and the HTGR cases using 100 million neutrons. The calculation times presented in Table III are total CPU times in minutes. All the calculations were calculated using one 2.4 GHz Intel Core i5 CPU.

**Table III. Total CPU times of the simulations.**

Pin-cell			HTGR		
Case	Time	Ratio	Case	Time	Ratio
Serpent 2, explicit	1585.4	2.28	Serpent 2, explicit	3497.0	4.20
Serpent 2, optimiz. mode 2	696.3	1.00	Serpent 2, optimiz. mode 2	830.9	1.00
Serpent 1.1.16+DBRC	463.0	0.66	Serpent 1.1.16+DBRC+FGT	911.7	1.10
Serpent 1.1.16	425.9	0.61	Serpent 1.1.16	845.6	1.02

## 5. CONCLUSIONS

The present paper discusses the implementation of the explicit temperature treatment method, introduced in [1], to Monte Carlo Reactor Physics code Serpent. Also first results calculated with the method are presented in this paper. The method provides for modelling of arbitrary temperatures in neutron transport routines with only 0 K continuous-energy cross sections available. The explicit treatment method also provides inherently correct velocities for target nuclei that can be utilized when solving the kinetics of scattering events.

Results for two test cases, a PWR pin-cell and a HTGR system, are presented in Section 4. The results calculated with the explicit method are in very good agreement with the reference.

Differences in the multiplication factors are lost in statistical deviation in both of the test cases.

In the PWR pin-cell case the differences in neutron flux remain smaller than 0.003 throughout the whole energy spectrum excluding the very low energies with poor statistics (Figure 2). Since the Doppler-preprocessor of Serpent was used to adjust the cross section temperatures in the reference case, the expected amount of error in the cross section reconstruction is higher than that of the basis library (0.001). This, together with the fact that the 0 K cross section of  $^{238}\text{U}$  is reconstructed to 0.003 tolerance, explains the deviances observed in the flux spectra.

The slightly smaller differences seen in the HTGR spectra (Figure 3) support the previous conclusion. In this case the reference was calculated using unmodified NJOY cross sections for which the reconstruction tolerance is known to be exactly 0.001. In this case the differences in flux spectra are smaller than 0.002 if the high and low energy regions with low statistics are ignored. Especially in the HTGR case the importance of DBRC is easy to notice: the resonance absorption would be clearly underestimated if DBRC was not used in the calculation of reference results.

The efficiency of the explicit treatment method depends strongly on the rejection sampling efficiency in Equation (11). This, in turn, depends on the material maximum temperature used in the generation of the majorant. The higher the temperature, the larger the majorant cross section and, consequently, the higher the proportion of rejected collision points.

This can be also observed in the performance measures presented in Table III. In the pin-cell case, where the temperatures ranged from about 550 K to 1300 K the calculation took 2.3 times more time than Serpent 2 with optimization mode 2. In the HTGR case, where the fuel was in 1800 K and other solid materials in 1200 K temperature, the calculation time ratio was significantly higher 4.2. The performance of the method could be improved by optimizing the group structure of the majorant cross sections or by changing to continuous-energy majorants. The present implementation with 40000 equi-lethargy groups is most likely far from optimal.

As it was observed, the usage of the explicit treatment method slows down the transport calculation notably. However, the slow-down is of tolerable magnitude and the method can be considered well-feasible to practical calculations, at least what comes to its efficiency. More efficient implementation of the method requires future work, and so does the usage of flux and reaction rate estimators with continuously-varying temperature profiles that are needed to take full advantage of the method. The explicit treatment method should also be made compatible with the thermal scattering laws and unresolved region probability table treatment before it can be utilized on full scale. It should, however, be noted that it is possible to use the explicit thermal treatment for only part of the materials in the problem geometry. The problem thus exists only if thermal scattering laws or probability tables are required for the same materials for which the temperature treatment is used.

In summary, the explicit treatment proved accurate and fast enough for practical transport calculations. The method, however, requires more research to extend its capabilities to the thermal and unresolved resonance regions that are essential when simulating realistic reactors. Already now the method is a great tool for examining different temperature-related phenomena such as temperature-dependent scattering kernels.

## ACKNOWLEDGEMENTS

This work was funded from the KÄÄRME project under the Finnish Research Programme on Nuclear Power Plant Safety SAFIR2014.

## REFERENCES

- [1] T. Viitanen and J. Leppänen, "Explicit Treatment of Thermal Motion in Continuous-energy Monte Carlo Tracking Routines," *Nuc. Sci. Eng.*, in-press.
- [2] B. Becker, R. Dagan and G. Lohnert, "Proof and implementation of the stochastic formula for ideal gas, energy dependent scattering kernel," *Ann. Nucl. Energy*, **36**, pp. 470–474 (2009).
- [3] R. E. MacFarlane and D. W. Muir, "NJOY99.0 Code System for Producing Pointwise and Multigroup Neutron and Photon Cross Sections from ENDF/B Data," PSR-480, Los Alamos National Laboratory (2000).
- [4] T. Mori, K. Okumura, Y. Nagaya and M. Nakagawa, "Application of continuous energy Monte Carlo code MVP to burn-up and whole core calculations using cross sections at arbitrary temperatures," *Proc. M&C'99*, Madrid, Spain, September 27–30, pp. 987–996, (1999).
- [5] J. Leppänen and T. Viitanen, "New Data Processing Features in the Serpent Monte Carlo Code", *J. Korean Phys. Soc.*, **59**, 1365–1368 (2011).
- [6] T. H. Trumbull, "Treatment of Nuclear Data for Transport Problems Containing Detailed Temperature Distributions," *Nucl. Technology*, **156**, 75–86 (2006).
- [7] G. Yesilyurt, W. R. Martin and F. B. Brown, "On-the-fly Doppler Broadening for Monte Carlo Codes," *Proc. M&C 2009*, Saratoga Springs, New York, May 3–7 (2009).
- [8] Serpent website, <http://montecarlo.vtt.fi> [referenced 27.10.2011]
- [9] MCNP X-5 Monte Carlo Team, "MCNP — a General Monte Carlo N-Particle Transport Code," Version 5, LA-UR-03-1987, Los Alamos National Laboratory (2003).
- [10] D. E. Cullen, "Program SIGMA1 (version 79-1): Doppler broaden evaluated cross sections in the evaluated nuclear data file/version B (ENDF/B) format," UCRL-50400 Part B., Lawrence Livermore National Laboratory (1979).
- [11] V. Tulkki. "ENIGMA State of the Art Report.", VTT Research Report VTT-R-09938-10, Technical Research Centre of Finland VTT (2010).
- [12] W. J. Kilgour, "The ENIGMA Fuel Performance Code, Users Guide, Version 5.8d", TD/NS/REP/0034, Berkeley Nuclear Laboratories (1992).
- [13] M. D. DeHart and A. P. Ulses, "Benchmark Specification for HTGR Fuel Element depletion", NEA/NSC/DOC(2009)13, Nuclear Energy agency, Organization for Economic Cooperation and Development (2009).
- [14] J. Leppänen and A. Isotalo, "Burnup Calculation Methodology in the Serpent 2 Monte Carlo Code", *Proc. PHYSOR 2012*, Knoxville, Tennessee, April 15–20 (2012).